

1 **Mitochondrial dysfunction and autophagy responses to skeletal muscle stress**

2

3 Anna S. Nichenko^{1,2}, W. Michael Southern^{1,2}, Anita E. Qualls², Alexandra B. Flemington², Grant

4 H. Mercer², Amelia Yin^{3,4}, Hang Yin^{3,4}, Jarrod A. Call^{1,2*}

5

6

7 ¹ Department of Kinesiology, University of Georgia, Athens, GA 30602, USA

8 ² Regenerative Bioscience Center, University of Georgia, Athens, GA 30602, USA

9 ³ Center for Molecular Medicine, University of Georgia Athens, GA 30602, USA

10 ⁴ Department of Biochemistry and Molecular Biology, University of Georgia, Athens, GA

11 30602, USA

12

13 **Running title: Autophagy and mitochondrial repair**

14

15 *Author to whom correspondence should be addressed:

16 Jarrod A. Call, PhD, 330 River Road, Ramsey Center, Department of Kinesiology, University of

17 Georgia, Athens, GA 30602, USA; E-mail: call@uga.edu, Tel: +1-706-542-0636, Fax: +1-706-

18 542-3148

19

20 Word count:

21 Number of figures 7

22

23

24 **Abstract**

25 Autophagy plays an important role in mitochondrial maintenance, yet many details of skeletal
26 muscle autophagic activity are unresolved in the context of muscle stress and/or damage.
27 Skeletal muscles from mice were stressed either by fatiguing contractions, eccentric contraction-
28 induced injury (ECCI), or freeze injury (FI) to establish a timeline of mitochondrial function and
29 autophagy induction after different forms of muscle stress. Only FI was sufficient to elicit a
30 reduction in mitochondrial function (-88%, $p=0.006$), yet both ECCI and FI resulted in greater
31 autophagy-related protein content (28-fold, $p\leq 0.008$) suggesting a tunable autophagic response.
32 Muscles from another cohort of mice were used to determine specific forms of autophagy, i.e.,
33 flux and mitochondrial-specific, in response to muscle damage. Mitochondrial-specific
34 autophagy was evident by accumulation of autophagy-related proteins in mitochondrial-enriched
35 muscle fractions following FI (37-fold, $p=0.017$); however, autophagy flux, assessed by LC3II
36 accumulation with the lysosomal inhibitor chloroquine, was insignificant suggesting a
37 physiological bottleneck in the clearance of dysfunctional organelles following FI. Ulk1 muscle-
38 specific knockout (Ulk1 MKO) mice were used to determine if autophagy is necessary for the
39 recovery of mitochondrial function after muscle damage. Ulk1 MKO mice were weaker (-12%,
40 $p=0.012$) and demonstrated altered satellite cell dynamics (e.g., proliferation) during muscle
41 regeneration after FI compared to littermate control mice, but determination of autophagy
42 necessity for the recovery of mitochondrial function was inconclusive. This study concludes that
43 autophagy is a tunable cellular response to muscle damaging stress and may influence muscle
44 fiber regeneration through interaction with satellite cells.

45

46

47 **Key Points Summary**

- 48 • Muscle contractility dysfunction is well characterized after many different types of
49 muscle stress however, the timing and magnitude of mitochondrial dysfunction and
50 autophagy induction after different types of muscle stress is largely unknown.
- 51 • In this study we found that only traumatic freeze injury causes mitochondria dysfunction
52 compared to fatigue contractions and eccentric contraction-induced injury, and that the
53 autophagic response to muscle stress scales to the magnitude of muscle damage, i.e.,
54 freeze vs. eccentric contraction-induced injury.
- 55 • We determined that total autophagy-related protein content has a greater response to
56 muscle fiber damage compared to autophagy flux likely reflecting a bottleneck of
57 autophagosomes awaiting degradation following muscle injury.
- 58 • Using a skeletal muscle-specific autophagy knockout mouse (Ulk1), we found that
59 muscle contractility and satellite cell activity might be influenced by cellular events
60 within the adult muscle fiber following muscle damage.

61

62

63

64

65 **Introduction**

66 The time course of muscle contractility loss after multiple types of muscle injury has
67 been well documented (6, 22, 27, 39, 40), but the timing and severity of mitochondrial
68 dysfunction after injury is largely unknown. Elucidating the loss and recovery of mitochondrial
69 function is important because mitochondria provide crucial energy for satellite cell proliferation
70 and differentiation, for the remodeling of damaged muscle fibers, and for the repair of initial
71 membrane disruption (13, 37). Mitochondria are affected by muscle fiber damage, as we and
72 others have reported a decrease in mitochondrial content and a subsequent rise in mitochondrial
73 biogenesis during muscle regeneration (6, 9, 27, 36). However, the approximation of
74 mitochondrial function using markers of mitochondrial content and biogenesis are inadequate to
75 characterize mitochondrial function particularly when evaluating pathological conditions (23).
76 Mitochondrial function is most appropriately analyzed by assessing the organelle's ability to
77 consume oxygen (i.e., mitochondrial respiratory function), and a primary goal of this study was
78 to investigate the time course of mitochondrial dysfunction and recovery after various forms of
79 muscle fiber stress.

80 Traditionally, the most physiologically-relevant marker of muscle fiber stress is a
81 temporary or prolonged loss of contractility. There are many different types of muscle stressors
82 that induce a temporary or prolonged loss of contractility (i.e. fatigue, eccentric contraction-
83 induced injury, contusion, freeze injury, myotoxic injury, burn injury, and volumetric muscle
84 loss injury) and, consequently, the severity and mechanism of reduced muscle contractility is
85 unique for each stressor (39). Severe stressors, such as freeze or myotoxic injuries, destroy the
86 contacted muscle fibers predominately by damaging the sarcolemma and disrupting
87 intramuscular ion homeostasis which leads to a 65%-80% loss of contractility (14, 21, 39).

88 Mitochondrial content follows a similar decline after these severe stresses (6, 27, 36), but the
89 functional deficit (i.e., mitochondrial respiration) has not been adequately investigated. Less
90 severe muscle stressors, like eccentric contraction-induced injuries, mainly disrupt excitation-
91 contraction coupling and result in an initial 40%-60% decline in muscle contractility (38). There
92 have been conflicting reports of mitochondrial oxygen consumption rates after downhill
93 treadmill running, a mild and indirect form of eccentric contraction-induced injury in mice with
94 some reporting no changes in mitochondrial respiration and others reporting transient changes
95 immediately and up to 48 hours after the injury (24, 30, 31, 33). Additionally, this injury model
96 is reported to elicit oxidative damage in the form of a greater presence of protein carbonyls and
97 oxidized lipids that could implicate mitochondrial dysfunction (26, 33). Finally, even a mild
98 muscle stressor such as muscle fatigue has been suggested to cause mitochondrial damage. Laker
99 & Drake et al. recently published that horizontal treadmill running was associated with greater
100 oxidation of the *pMitoTimer* reporter gene tagged to the Tyr-65 residue of Cytochrome C
101 Oxidase subunit VIII (20), indicative of mitochondrial oxidative damage. Therefore, it is
102 apparent that multiple types of muscle stressors may induce unique mitochondrial responses,
103 although how relevant these are to mitochondrial function after muscle stress is unknown.

104 We have previously highlighted that when mitochondria are stressed or damaged a
105 primary cellular mechanism for maintaining the quality of the mitochondria network is
106 macroautophagy (6, 27). Macroautophagy (hereafter referred to as autophagy) is a cellular
107 process which degrades dysfunctional organelles and proteins into their original amino acid and
108 fatty acid components to be recycled in the cell. The Ulk1 (Unc-51 like autophagy activating
109 kinase 1) complex initiates autophagy by signaling the Beclin1 (Atg6) complex to convert
110 microtubule-associated protein light chain B I (LC3I) into LC3II, which then forms a double-

111 membrane vesicle called an autophagosome. Autophagosomes encapsulate damaged organelles
112 or proteins and eventually fuse with a lysosome to undergo degradation. Conventionally,
113 measurements of Beclin1 or LC3 protein contents have been used to characterize broad changes
114 in autophagy after various muscle stressors, but autophagy is a dynamic process that can be
115 affected at many different stages, therefore the static measurements of Beclin1 and LC3 fail to
116 capture the changes in overall autophagic flux (i.e., ongoing autophagic degradation) (17).
117 Furthermore, the specific degradation of mitochondria by autophagy, alternatively defined as
118 mitophagy, has primarily been investigated through localization of mitochondrial markers and
119 LC3 puncta in skeletal muscle after treadmill running (20). There is currently a knowledge gap in
120 the literature regarding the extent to which muscle fiber damage results in greater autophagy
121 flux, and whether autophagy contributes to elimination of damaged mitochondria. Understanding
122 the specific role of autophagy after muscle fiber damage may be leveraged to develop targeted
123 therapeutic modalities to address muscle regeneration in conditions such as aging and muscular
124 dystrophy where deficits in muscle repair and autophagy have been reported (25, 29, 32).

125 The objectives of this study were: 1) to elucidate the relationship between mitochondrial
126 dysfunction and autophagy induction after different types of muscle stress; 2) to determine the
127 extent to which autophagy flux and mitochondrial specific autophagy respond to muscle fiber
128 stress; and 3) to determine if Ulk1-mediated autophagy is necessary for the recovery of
129 contractile and mitochondrial function after muscle damage. We hypothesized that autophagy
130 responses would scale to the magnitude of muscle stress, that autophagy flux and mitochondrial-
131 specific autophagy would contribute to the autophagy response to muscle stress, and that Ulk1-
132 mediated autophagy would be necessary for the recovery of muscle contractility and
133 mitochondrial function after muscle stress.

134 **Methods**

135

136 ***Ethical Approval***

137 All animal protocols were approved by the University of Georgia Animal Care and Use

138 Committee under the national guidelines set by the Association for Assessment and

139 Accreditation of Laboratory Animal Care.

140 ***Animal Models***

141 Male and female C57BL/6J mice aged 3-4 months were bred in-house and housed 5 per

142 cage in a temperature-controlled facility with a 12:12 hour light:dark cycle. Muscle-specific

143 Ulk1 knockout mice (Ulk1 MKO) with *myogenin-Cre* and LoxP flanked *Ulk1* and their

144 *myogenin-Cre* negative littermates (LM) were used to test the necessity of Ulk1 for

145 mitochondrial function and strength recovery after traumatic freeze injury. All mice had *ad*

146 *libitum* access to food and water throughout the experiments.

147 ***Experimental Design***

148 The first cohort of wildtype C57BL/6J mice were used to assess the time course of

149 mitochondrial function and autophagy induction after various muscle stressors. Briefly, mice

150 were randomized into 3 groups; (i) a non-damaging metabolically fatiguing challenge (n=12), (ii)

151 eccentric contraction-induced injury (n=20), and (iii) traumatic freeze injury (n=28). Tissues

152 were analyzed for mitochondrial function, mitochondrial content, and autophagy induction

153 immediately, 6 hours, and one day post for all groups. No additional time points were assessed

154 for the fatigue group because initial data indicated there were no significant changes (Fig. 1 & 2).

155 Additional time points, 3 and 7 days post, were assessed for the eccentric-contraction induced

156 and freeze injury groups to characterize changes in mitochondrial function during the first week

157 of recovery.

158 The second cohort of wildtype C57BL/6J mice were used to analyze autophagy flux and
159 mitochondrial-specific autophagy following traumatic freeze injury based on results from the
160 first cohort. Unilateral freeze injuries were performed on all mice before randomization into two
161 groups. One group (n=12) was used for an autophagy flux assay where half of the mice received
162 chloroquine to inhibit lysosomal degradation (17) and the other half were treated with saline 7
163 days after injury. Injured and contralateral limbs were collected and immunoblots for autophagic
164 flux (LC3 II accumulation) were performed. The second group (n=8) was sacrificed 7 days after
165 injury and a differential centrifugation protocol was done on both injured and contralateral
166 uninjured limbs to determine the accumulation of autophagy-related proteins in mitochondria-
167 enriched versus cytosolic fractions.

168 The third cohort of mice included Ulk1 MKO and LM mice to test the necessity of Ulk1
169 for recovery of mitochondrial function after injury (n=20) (10, 16, 18). Prior to injury, peak-
170 isometric dorsiflexion torque measurements were performed on Ulk1 MKO and LMs.
171 Immediately following, mice underwent unilateral freeze injuries and peak-isometric
172 dorsiflexion torque measurements were performed again 14 days post. Mice were sacrificed
173 afterwards, and muscle tissue was harvested for mitochondrial function, mitochondrial content,
174 and autophagy-related protein analyses. The selection of 14 days after injury was based on the
175 results from cohort 1 showing mitochondrial function was less than one-third of uninjured at 7
176 days after injury (Fig. 1), and results from our previous studies indicating 14 days is sufficient to
177 observe differences in mitochondrial content with insufficient autophagy (6, 27)

178 ***Metabolic Fatiguing Protocol***

179 Mice were anesthetized using 1-2% isoflurane in oxygen, and left hind limb was shaved
180 and aseptically prepared. The foot was positioned into a foot-plate attached to the servomotor

181 (Model 129 300C-LR; Aurora Scientific, Aurora, Ontario, Canada) where the ankle joint was
182 adjusted to a 90° angle and secured at the knee joint. Platinum-Iridium (Pt-Ir) needle electrodes
183 were inserted percutaneously on both sides of the peroneal nerve and the testing platform was
184 maintained at 37°C throughout the optimization and muscle stressor protocols. Optimal muscle
185 stimulation was achieved by finding peak-isometric torque of the ankle dorsiflexors (tibialis
186 anterior (TA), extensor digitorum longus (EDL), extensor hallucis longus muscles) through
187 increasing the current stimulating the peroneal nerve at a 200 Hz pulse frequency prior to
188 executing the muscle stressor protocol. The fatiguing protocol consisted of 30 minutes of
189 continuous 10Hz stimulation which was modeled after muscle activation during a 30 minute
190 treadmill run (3).

191 ***Eccentric Contraction-Induced Injury***

192 Mice were prepared, optimal muscle stimulation was verified following the methods
193 listed above, and eccentric contraction-induced injury protocol was executed as previously
194 described (4, 5). Briefly, for the eccentric contraction-induced injury, the foot was passively
195 moved from the 0° position (perpendicular to the tibia) to 20° of dorsiflexion. The ankle
196 dorsiflexor muscles were stimulated at 200 Hz for a 100-ms isometric contraction followed by an
197 additional 50-ms stimulation while moving from 20° dorsiflexion to 20° plantarflexion at an
198 angular velocity of 2000°/s. Eccentric contractions were repeated every 10 seconds until a total
199 of 100 electronically stimulated eccentric contractions were complete.

200 ***Freeze Injury***

201 Freeze injury was performed as previously described (39). Before surgery, mice were
202 anesthetized using isoflurane and given a local anesthetic injection of bupivacaine (5mg/kg)(17).
203 Afterwards, the left limb was aseptically prepared, a 1.5cm incision was made over the TA

204 muscle, and a steel probe cooled with dry ice was applied to the belly of the TA for 10 seconds.
205 Upon completion of the freeze injury, the incision was closed with nylon suture and mice were
206 administered meloxicam (2mg/kg) for pain management immediately and again 12 hours after
207 surgery (39).

208 *Oxygen Consumption Rates*

209 Mitochondrial function was assessed in dissected permeabilized muscle fiber bundles
210 from both the stressed and contralateral control limb using methods adapted from Kuznetsov et
211 al. and as we have previously described (19, 34). To ensure we were testing homogenously
212 stressed muscle fibers, entire EDL muscles were permeabilized for the eccentric contraction-
213 induced injury and fatiguing protocol and TA muscle fibers were dissected from the affected area
214 for the freeze injury group. Oxygen consumption rates were made through the use of a Clark-
215 type electrode (Hansetech) kept at a constant 25°C with constant stirring. State III respiration
216 was accomplished by addition of glutamate (10mM), malate (5mM), succinate (10mM), and
217 ADP (5mM). Oxygen consumption rates during State III respiration were normalized to tissue
218 mass loaded into chamber.

219 *Enzyme Assays*

220 Both citrate synthase (CS) and succinate dehydrogenase (SDH) enzyme assays were
221 performed to quantify mitochondrial content in the stressed and contralateral control limbs after
222 muscle fatigue, eccentric contraction-induced injury, and freeze injury. The portion of muscle
223 remaining after fiber dissection for oxygen consumption rates was weighed and homogenized in
224 33mM phosphate buffer (pH 7.4) at a muscle to buffer ratio of 1:40 using a glass tissue grinder.
225 Citrate Synthase activity was measured from the reduction of DTNB overtime as previously

226 described (27). Succinate Dehydrogenase activity was measured from the reduction of
227 cytochrome c as previously described (12).

228 ***Immunoblot***

229 For autophagy-related protein content analysis, protein was extracted from stressed and
230 contralateral control muscles. 25 µg of total protein was separated by SDS-PAGE, transferred
231 onto a PVDF membrane, and immunoblotted as previously described (27). The following
232 antibodies (Cell Signaling, Danvers, MA) were used: Ulk1 (1:10000), beclin-1 (1:1000), and
233 LC3B (1:1000). Immunoblots were normalized to total protein in lane and quantified using Bio-
234 Rad Laboratories Image Lab software (Hercules, CA) (8, 35, 44).

235 ***Chloroquine Treatment***

236 In order to measure autophagy flux after injury we used a lysosomal inhibitor,
237 chloroquine, as recommended by the autophagy guidelines (17). Mice underwent freeze injuries
238 as described above and recovered for 7 days. Two hours before sacrifice mice were given an
239 intraperitoneal injection of chloroquine (65mg/kg) to inhibit autophagosome degradation. TA
240 muscle tissue was harvested and immunoblots for LC3II quantification were carried out as
241 described above.

242 ***Differential Centrifugation***

243 To obtain mitochondrial-enriched fractions and cytosolic fractions, differential
244 centrifugation was performed on injured and contralateral uninjured TA muscles 14 days after
245 injury as described (20). Briefly, muscles were homogenized in fractionation buffer [20 mM
246 HEPES, 250 mM Sucrose, 0.1 mM EDTA, plus protease and phosphatase] in a glass tissue
247 homogenizer at a 1:20 tissue to buffer ratio. Homogenates were then spun at 800×g for 10 min at
248 4°C, supernatant was removed and then spun at 9000×g for 10 min at 4°C. The supernatant was

249 again removed and resuspended in an equal volume of 2x Laemmli buffer resulting in the
250 cytosolic fraction. The remaining mitochondrial pellets were resuspended in fractionation buffer
251 then spun at 11,000×g for 10 min at 4°C. Resulting mitochondrial-enriched pellets were
252 resuspended in 20 µl of 2x Laemmli buffer resulting in the mitochondrial-enriched fraction. Both
253 fractions were boiled for 5 min at 97°C, then frozen at –80°C until immunoblot analysis.

254 ***Immunofluorescent staining for satellite cells***

255 Satellite cell dynamics were evaluated as previously described (42). Briefly, injured
256 muscles from Ulk1 MKO mice (n=3) and LM mice (n=3) were isolated at 10 days post-injury
257 and subjected to cryo-sectioning. Muscle sections were stained with primary antibody, Pax7 (1:5;
258 DSHB) and Ki67 (1:1000; Abcam) overnight at 4 degrees, followed with a secondary antibody
259 stain at room temperature for 1 hour. To evaluate satellite cell dynamics, muscle cross-sections
260 (at 3 representative levels) were used to enumerate the total number of satellite cells (Pax7+),
261 proliferating satellite cells (Pax7+/Ki67+), and self-renewing satellite cells (Pax7+/Ki67-).

262 ***Statistics***

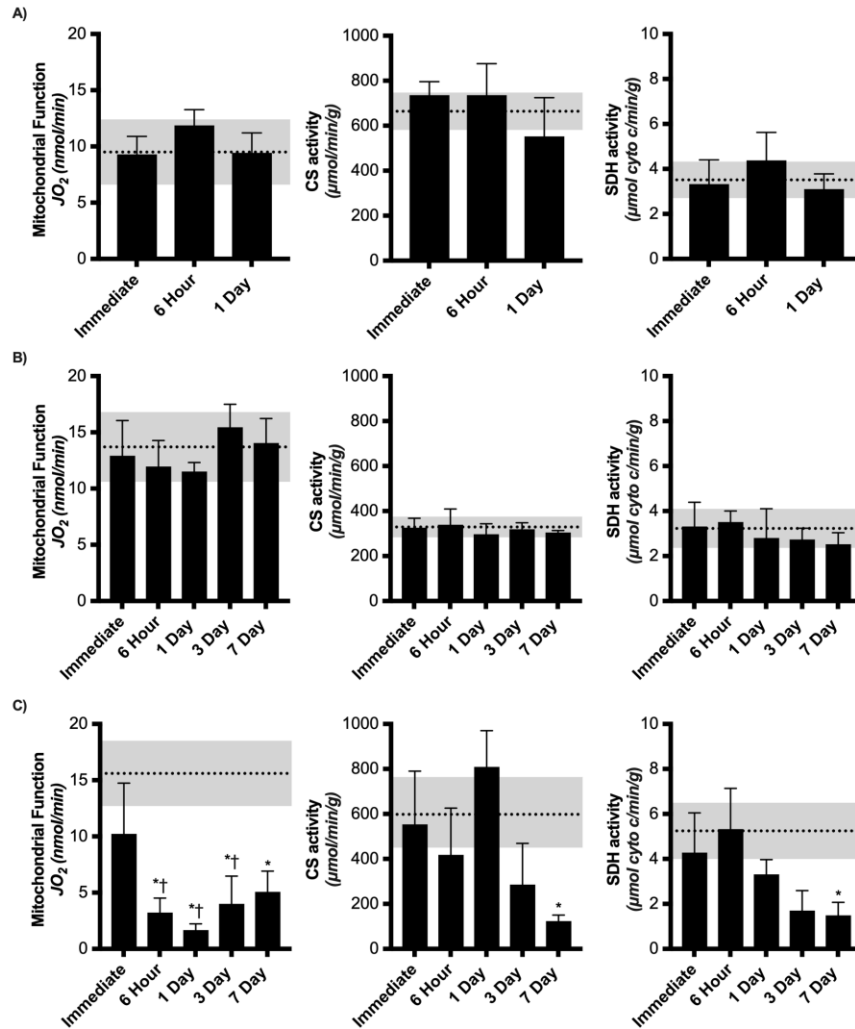
263 Differences in mitochondrial function, mitochondrial content and autophagy protein
264 expression after different muscle stressors were analyzed by two-way repeated measures (RM)
265 analysis of variance (ANOVA) with the repeated measures being the injured vs. uninjured
266 contralateral control limb and the other factor being time. Autophagy flux immunoblots were
267 analyzed by two-way RM ANOVA with the repeated measures being the injured vs. uninjured
268 contralateral control limb and the other factor being treatment (saline or chloroquine).
269 Differential centrifugation immunoblots were analyzed by two-way RM ANOVA with the
270 repeated measures being the injured vs. uninjured contralateral control limb and the other factor
271 being fraction (mitochondria-enriched or cytosolic). Ulk1 KO and LM comparisons were

272 analyzed by two-way RM ANOVA with the repeated measures being the injured vs. uninjured
273 contralateral control limb and the other factor being genotype. All data were required to pass
274 normality (Shapiro-Wilk) and equal variance tests (Brown-Forsythe F test) before proceeding
275 with the two-way RM ANOVA. Significant interactions were tested with Tukey's *post hoc* test
276 using JMP statistical software (SAS, Cary, NC) to find differences between groups. Group main
277 effects are reported where significant interactions were not observed. An α level of 0.05 was
278 used for all analyses and all values are means \pm SD.
279

280 **Results:**

281 **Time course of mitochondrial dysfunction and content after different muscle stressors**

282 Across all conditions of muscle stress, there was no effect of time on mitochondrial function or
283 content in the contralateral control limb ($p \geq 0.55$) therefore only the collective mean (dashed line)
284 and standard deviations (grey region) are represented in each panel of Fig. 1. There was no
285 difference in mitochondrial function or enzyme content between stressed and contralateral
286 control limbs at any time point after the metabolic fatigue protocol (Main Effect: Limb, $p \geq 0.24$,
287 Fig. 1A). Similarly, there was no difference in mitochondrial function or content following the
288 eccentric contraction-induced injury protocol (Main Effect: Limb, $p \geq 0.17$, Fig. 1B).
289 Mitochondrial function was significantly decreased 6 hours after traumatic freeze injury (20% of
290 uninjured), continued to decline to its lowest functional capacity one day after injury (12% of
291 uninjured), and by seven days after injury had recovered to ~34% of uninjured control limbs
292 (Significant Interaction: $p = 0.006$, Fig. 1C). Mitochondrial content was not significantly different
293 from contralateral control limbs until day 7 post-injury (Significant Interaction, $p \leq 0.021$, Fig.
294 1C) suggesting a disproportionate loss of mitochondrial function early after freeze injury.



296

297 **Figure 1. Mitochondrial function and content changes over time after different muscle stressors.**

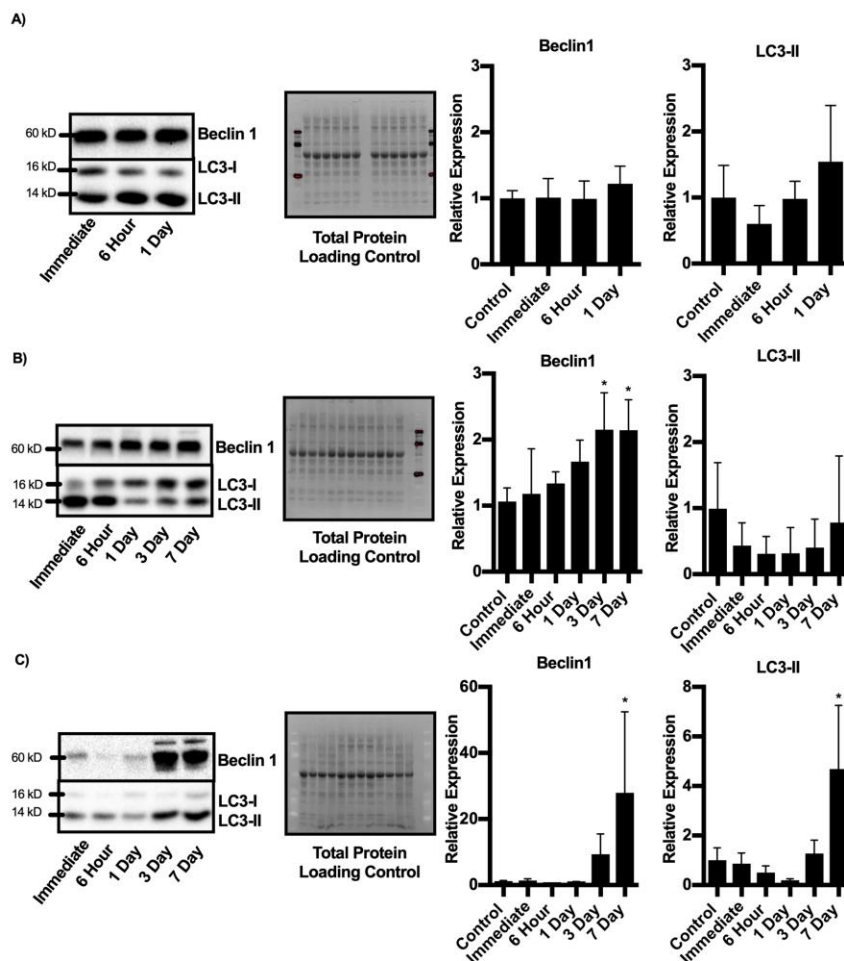
298 Mitochondrial function was assessed by oxygen consumption measurements of permeabilized TA or EDL muscle
299 fibers and mitochondrial content was assessed by mitochondrial enzyme assays of citrate synthase (CS) and
300 succinate dehydrogenase (SDH) activity immediately, 6 hours, 1, 3, and 7 days after A) fatiguing protocol (n=12),
301 B) Eccentric contraction-induced injury (n=20), C) and traumatic freeze injury (n=28). Dashed line represents
302 average contralateral control limb and shaded grey regions are \pm SD. Stressed limb data are presented as \pm
303 SD. * Significantly different from uninjured, † significantly different from immediate injured.

304

305

306 Time course of autophagy induction after different muscle stressors

307 Immunoblots of Beclin1 and LC3II were analyzed to determine the time course of autophagy
308 induction after different muscle stressors. There was no change in relative expression of Beclin1
309 or LC3II in the stressed limb compared to the control limb after the fatiguing protocol ($p \geq 0.728$,
310 Fig. 2A). Beclin1 expression increased 2-fold at 3 days after the eccentric contraction-induced
311 injury and remained elevated through 7 days post injury (Significant Interaction, $p = 0.014$, Fig.
312 2B), however, no significant change was observed with LC3II ($p = 0.9023$). In contrast, traumatic
313 freeze injury resulted in a robust autophagy induction evident by a 28-fold increase in Beclin1
314 expression and a 5-fold increase in LC3II at 7 days after injury ($p \leq 0.008$, Fig. 2C).

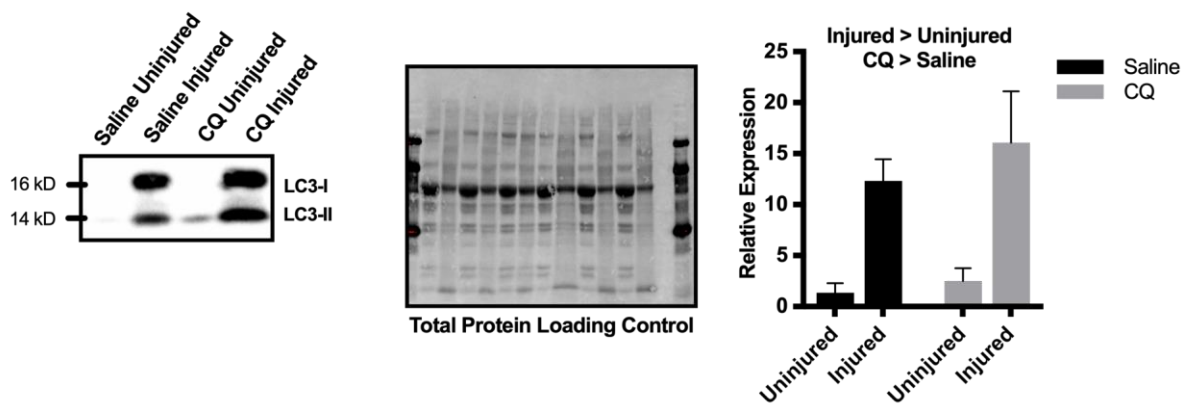


316 **Figure 2. Autophagy related protein expression after different muscle stressors.** Representative immunoblot
317 and semi-quantitative analysis of Beclin1 and LC3II relative expression compared to control uninjured limb
318 immediately, 6 hours, 1, 3, and 7 days after A) fatiguing protocol (n=12), B) Eccentric contraction-induced injury
319 (n=20), C) traumatic freeze injury (n=28). * significantly different from control limb. Blots are normalized to total
320 protein as a loading control and presented as relative expression to control uninjured limbs. Data are presented as
321 means \pm SD.

322

323 **Autophagy flux response after traumatic freeze injury**

324 Static measurements of autophagy-related proteins are a poor indicator of dynamic autophagy
325 activity, therefore, we measured autophagy flux by quantifying LC3II accumulation after
326 chloroquine (CQ) treatment in freeze injured muscle as this muscle stressor had the most robust
327 autophagy response (Fig. 2) (17). LC3II expression was increased nearly 14-fold in the injured
328 limb compared to the uninjured limbs at 7 days after injury as previously found (27) (Main
329 effect: Injury $p < 0.0001$, Fig. 3). Additionally, CQ treatment resulted in greater LC3II
330 accumulation independent of injury (Main effect: Treatment $p = 0.0178$, Fig. 3). These results
331 suggest that autophagy flux increases with muscle injury but does not appear to coordinate with
332 the robust response of autophagic machinery after traumatic freeze injury.



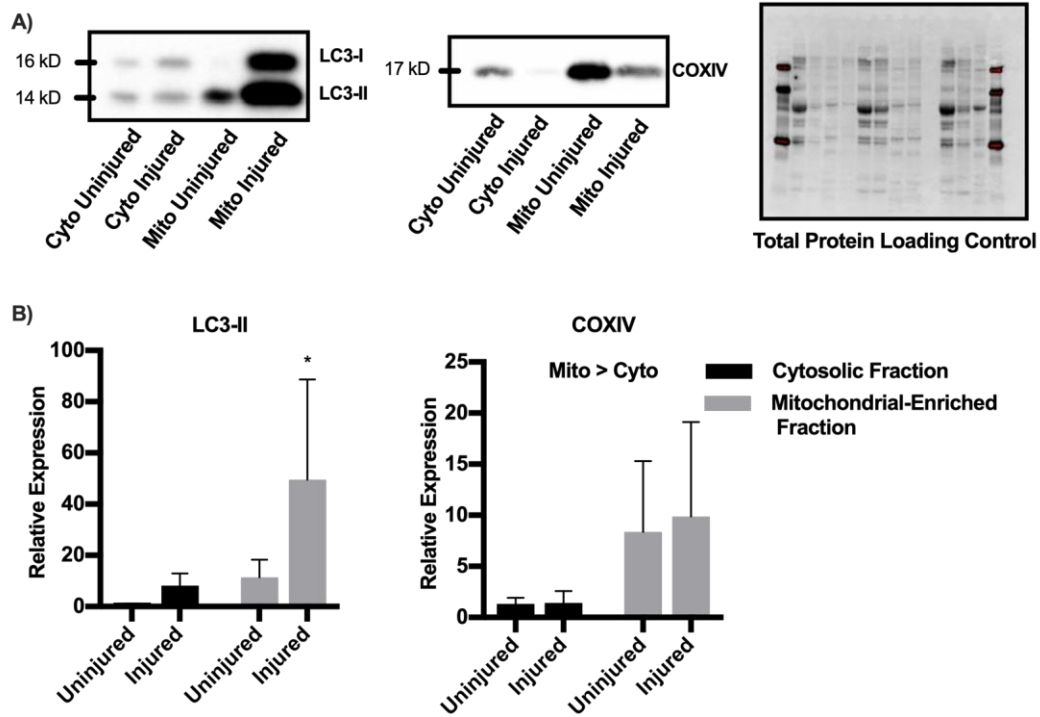
333

334 **Figure 3. Autophagy flux after traumatic freeze injury.** A) Representative immunoblot and semi-quantitative
335 analysis of relative LC3II expression in both injured and contralateral limbs from mice treated with saline (n=6) or
336 chloroquine (n=6) 7 days after freeze injury. Blots are normalized to total protein as a loading control and presented
337 as relative expression to uninjured limbs from saline treated mice. Data are presented as means \pm SD.

338

339 **Mitochondrial-specific autophagy after traumatic freeze injury**

340 Because autophagy induction appeared to accompany mitochondrial dysfunction after freeze
341 injury (Fig. 1 & 2), cytosolic fractions and mitochondrial-enriched fractions were subject to
342 immunoblot analysis of LC3II to elucidate the extent of mitochondrial-specific autophagy.
343 COXIV expression was increased 8-fold in the mitochondrial-enriched fractions compared to the
344 cytosolic fractions (COXIV Main Effect: Fraction, $p=0.049$, Fig. 4). Interestingly, LC3II
345 expression was 37 times greater in the injured mitochondrial-enriched fractions compared to the
346 injured cytosolic fractions suggesting a large mitochondrial-specific autophagy response to
347 traumatic freeze injury (Significant Interaction, $p=0.017$, Fig. 4), in agreement with previous
348 reports of accumulation of autophagy-related proteins at the mitochondria after physiological
349 muscle stress (6, 20).



350

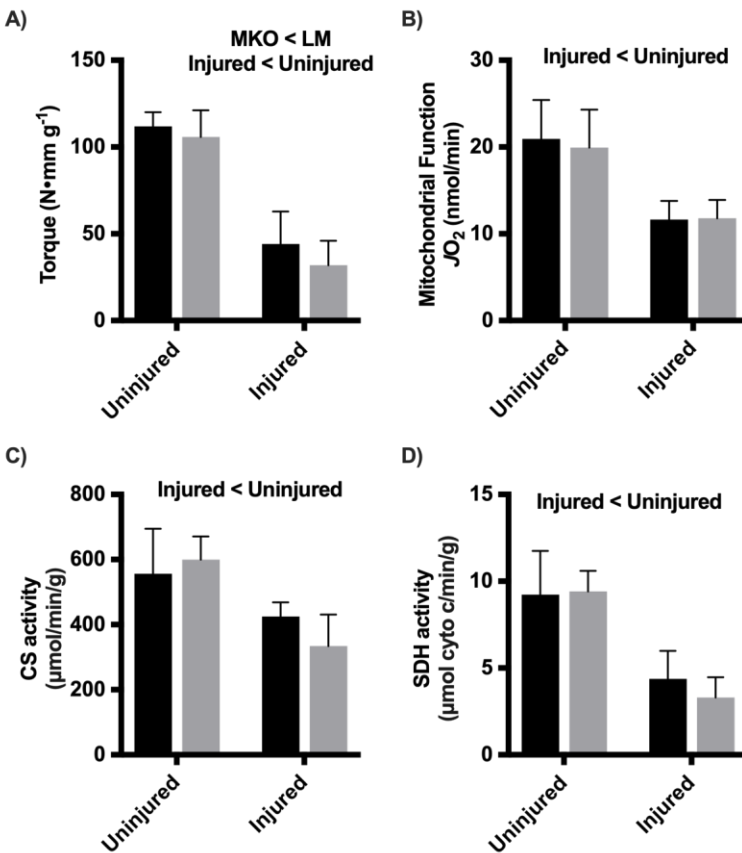
351 **Figure 4. Autophagy induction in mitochondrial-enriched fractions after freeze injury.** A) Representative
352 immunoblots and B) semi-quantitative analysis of LC3II expression and COXIV expression in cytosolic and
353 mitochondrial-enriched fractions from mice 7 days after freeze injury (n=8). Blots are normalized to total protein as
354 a loading control and presented as relative expression to uninjured cytosol fraction. * significantly different from all
355 other groups. Data are presented as means \pm SD.

356

357 **Recovery of strength, mitochondrial function, and mitochondrial content in Ulk1 MKO** 358 **mice after traumatic freeze injury**

359 Mitochondrial-specific autophagy is mediated by the autophagy-related protein Ulk1 (6). We and
360 others have investigated the role of Ulk1 following muscle stress and specifically mitochondrial
361 stress (20, 27) however, whether Ulk1 is required for the recovery of mitochondrial function
362 after injury has not been investigated. To ascertain the role of Ulk1-mediated autophagy in the
363 recovery of mitochondrial function, we compared Ulk1 MKO and LM mice (6). Peak-isometric
364 torque was significantly lower in Ulk1 MKO compared to LM mice independent of injury (-

365 12%, Main Effect: Injury and Genotype, $p \leq 0.012$, Fig 5A). Mitochondrial function was
366 decreased 43% in the injured limbs independent of genotype (Main Effect: Injury, $p < 0.0001$, Fig
367 5B), and mitochondrial content was reduced by 34% and 58%, CS and SDH respectively,
368 independent of genotype (Main Effect: Injury, $p \leq 0.0006$, Fig 5C, Fig 5D).



369
370 **Figure 5. Muscle torque, mitochondrial function, and mitochondrial content before and after injury in MKO.**

371 A) Comparison of MKO (n=10) and LM (n=10) dorsiflexion muscle torque before (uninjured) and 14 days after
372 freeze injury. B) Mitochondrial function assessed by oxygen consumption of permeabilized TA muscle in injured
373 and contralateral uninjured limbs 14 days after freeze injury. C) Mitochondrial content assessed by Citrate Synthase
374 activity and D) Succinate Dehydrogenase activity in TA muscles of LM and Ulk1 MKO mice in both injured and
375 contralateral control limbs.

376

377

378 **Autophagy-related protein induction in Ulk1 MKO mice after freeze injury**

379 LC3II expression increased more than 7-fold in the injured limbs compared to the uninjured

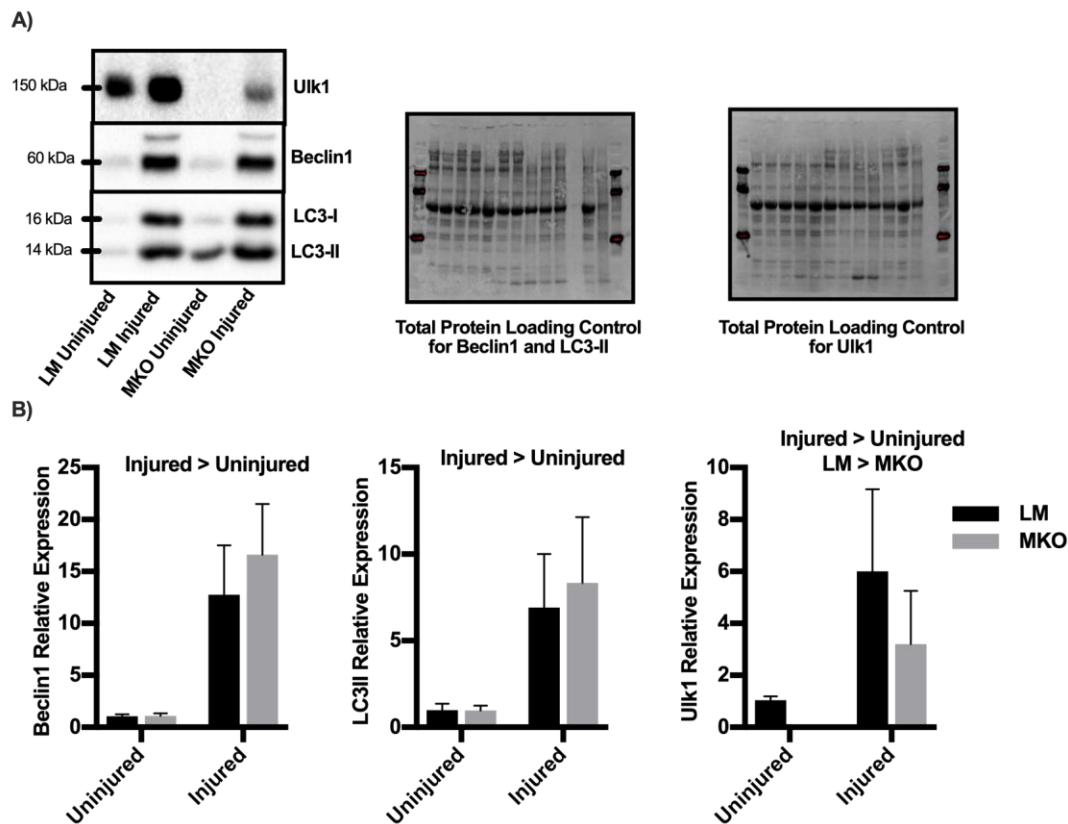
380 limb, independent of genotype (Main Effect: Injury, $p \leq 0.0001$, Fig 6B). Additionally, Beclin1

381 expression increased more than 14-fold with injury, independent of genotype (Main Effect:

382 Injury, $p \leq 0.0001$, Fig 6B). Prior to injury, Ulk1 MKO mice had no Ulk1 expression as expected,

383 however after injury both the LM and Ulk1 MKO mice had similar levels of Ulk1 protein

384 content (Main Effect: Injury and Genotype, $p \leq 0.042$, Fig 6B).



385

386 **Figure 6. Autophagy related protein induction after traumatic freeze injury.** A) Representative immunoblots

387 and B) semi-quantitative analysis of Beclin1, LC3II, and Ulk1 protein expression in both injured and contralateral

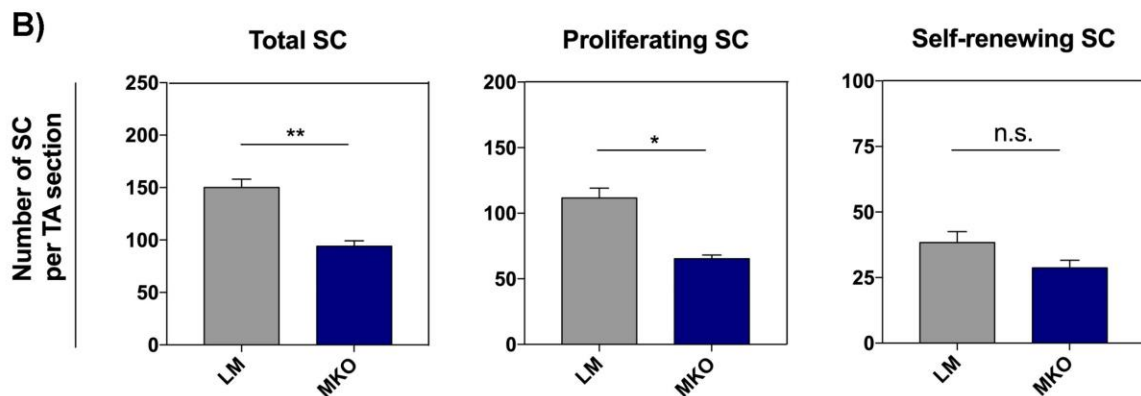
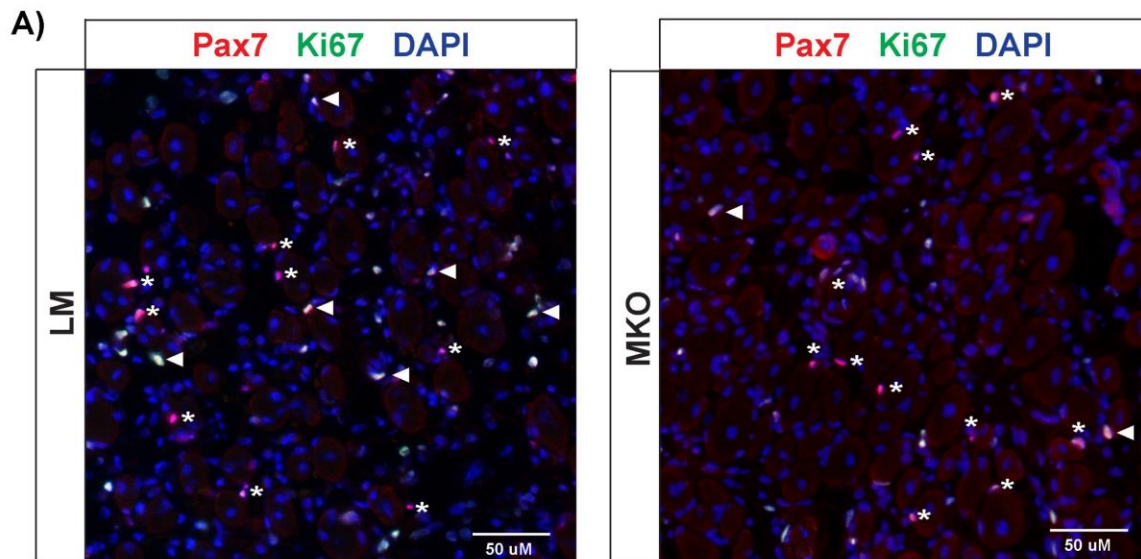
388 uninjured limbs of Ulk1 MKO (n=10) and LM (n=10) mice 14 days after freeze injury. Blots are normalized to total

389 protein as a loading control and presented as relative expression to LM uninjured limbs. Data are presented as means

390 \pm SD.

391 **Impaired satellite cell proliferation in Ulk1 MKO mice**

392 At the conclusion of our study we decided to explore satellite cell dynamics in Ulk1 MKO mice
393 because: (i) the strength deficit in the Ulk1 MKO mice, which is in agreement with our previous
394 reports (17), suggests Ulk1 knockout in myofibers impairs regenerative myogenesis and (ii)
395 satellite cells are essential stem cells for regenerative myogenesis in skeletal muscle. 10 days
396 post-injury there were a greater number of total and proliferating satellite cells in the freeze
397 injured muscles of LM compared to Ulk1 MKO mice ($p \leq 0.016$, Fig. 7), and no difference
398 between mice in the number of self-renewing satellite cells ($p = 0.140$, Fig. 7).



400 **Figure 7. Muscle-specific Ulk1 knockout impairs satellite cell proliferation after traumatic freeze injury.** A)
401 Representative immunofluorescence imaging of muscle cross-sections from LM (n=3) and Ulk1 MKO (n=3) mice at
402 10 days after injury. Arrowheads: Pax7⁺/Ki67⁺ proliferative satellite cells. Asterisks: Pax7⁺/Ki67⁻ self-renewing
403 satellite cells. B) Numbers of total, proliferating, and self-renewing satellite cells per muscle cross-section.

404

405 **Discussion**

406 A primary goal for this study was to address several knowledge gaps in the field related
407 to mitochondrial dysfunction after skeletal muscle stress, and the role of autophagy in mediating
408 a response between the two. Mitochondria are appreciated as contributing to the regenerative
409 potential, plasticity, and overall quality of skeletal muscle, and, therefore, investigating the
410 muscle fiber-mitochondrial relationship may produce important targets for rehabilitation and
411 disease prevention. However, there appear to be inconsistencies in the literature regarding what
412 types of muscle stressors elicit mitochondrial dysfunction (20, 30, 31, 33), as well as the extent
413 to which autophagy is necessary for the timely repair of mitochondrial dysfunction after muscle
414 stress (6). Herein, we relied upon oxygen consumption as the marker of mitochondrial function,
415 enzyme activities of succinate dehydrogenase and citrate synthase as markers of mitochondrial
416 content, and a muscle-specific Ulk1 knockout mouse to test the necessity of autophagy for the
417 recovery of mitochondrial function and content.

418 The first knowledge gap we explored was the extent to which three often utilized muscle
419 stressors (fatigue, eccentric contraction-induced injury, freeze injury) that produce a loss in
420 muscle contractility (21, 39) and an autophagic response (2, 6, 27) will cause mitochondrial
421 dysfunction, i.e., a decline in oxygen consumption. Reduced mitochondrial oxygen consumption
422 was only observed after traumatic freeze injury and was not decreased until 6 hours after injury
423 (Fig. 1) in stark contrast to the immediate ~70% loss in force production (39). Fatiguing

424 exercises and eccentric contraction-induced injury have been reported to cause mitochondrial
425 dysfunction (20, 26) in contrast to our findings. A likely explanation for these conflicting
426 findings may be the tools utilized to investigate mitochondrial dysfunction and/or damage.
427 Specifically, immunohistological techniques like confocal microscopy used by Laker & Drake et
428 al (20) are useful for mechanistic investigations into localized mitochondrial events but do not
429 necessarily reflect changes across the entire mitochondrial network; whereas oxygen
430 consumption measurements test the functional capacity of the entire mitochondrial reticulum but
431 do not capture more nuanced physiology such as fission and fusion events. It is irrefutable that
432 functional, biochemical, and immunohistological approaches can provide valuable insight into
433 mitochondrial physiology, yet when appropriate, future studies may consider the culminative
434 advantage of combining more than one technique to avoid further inconsistencies in the
435 literature.

436 Previous muscle damage research, including our own, has failed to investigate the
437 dynamic properties of autophagy after skeletal muscle injury. Specifically, our previous work (6,
438 27) and this current work (Fig. 2) shows that the autophagy-related protein response scales to the
439 magnitude of muscle damage after injury, but it remains unclear the extent to which autophagy
440 flux matches the increases in autophagy machinery. Autophagy flux is described as the rate at
441 which the entire process of autophagy occurs; meaning how quickly autophagosomes form
442 around damaged content, fuse with lysosomes and subsequently degrade (17). In contrast, an
443 increase in autophagy machinery is a static measurement and is not always connected to an
444 increase in autophagy flux. Static measurements of LC3II protein content are often used as
445 proxies for autophagy flux but can actually indicate (i) an inhibition in lysosomal fusion to the
446 autophagosome, (ii) inhibition of autolysosome degradation, (iii) an increase in the amount of

447 autophagosomes (without an increase in flux), or (iv) an increase in autophagy flux (17).
448 Therefore, in order to assess changes in autophagy flux after injury we used the lysosomal
449 inhibitor chloroquine and measured LC3II accumulation after blocking autolysosome
450 degradation. We found that autophagy flux does increase a modest amount (~1.5-fold increase)
451 but does not scale to the large influx of autophagy machinery (~6-fold increase) we observed
452 after traumatic freeze injury (Fig. 3). This disproportionately small increase in flux may
453 represent a limiting factor, or bottleneck, in the ability of autophagy to quickly clear away
454 damaged proteins and organelles, and serve as a novel target to expedite the healing process in
455 injured skeletal muscle.

456 We and others have previously reported that traumatic muscle injury results in a loss of
457 mitochondrial content (6, 9, 27, 36), and herein we report that it also results in a loss of
458 mitochondrial function (Fig. 1). A remaining question was the extent to which mitochondrial-
459 specific autophagy, sometimes referred to as mitophagy, participates in the clearing of
460 dysfunctional mitochondria after traumatic muscle injury. Laker & Drake et al. demonstrated that
461 mitochondrial-specific autophagy was critical for clearing damaged, i.e, ROS-producing
462 mitochondria after muscle fatigue (20); therefore, it is logical to hypothesize that mitochondrial-
463 specific autophagy may occur after a more severe muscle stressor such as traumatic muscle
464 injury in order to clear away the dysfunctional mitochondria. To address this knowledge gap, we
465 analyzed autophagy-related proteins in mitochondrial-enriched fractions and cytosolic fractions.
466 We found a robust accumulation of autophagy-related protein localized to the mitochondria after
467 freeze injury suggesting that autophagy does participate in the clearance of dysfunctional
468 mitochondrial after traumatic muscle injury (Fig. 4). This is the first study linking autophagy to

469 mitochondrial dysfunction in injured skeletal muscle and understanding the process of clearing
470 dysfunctional mitochondria after muscle injury may provide targets to facilitate muscle recovery.

471 In order to specifically test the extent to which mitochondrial-specific autophagy is
472 important for muscle recovery after traumatic muscle injury we utilized a Ulk1 MKO mouse
473 model. We and others have reported that Ulk1 may play an important role in both mitochondrial
474 function and strength recovery after injury (6, 27) . Our initial results suggested that Ulk1 is not
475 required for the recovery of mitochondrial function after freeze injury (Fig. 5); however, there is
476 a major consideration worth noting. Our Ulk1 MKO mouse model is a *myogenin-Cre* driven
477 gene knockout, meaning Ulk1 is not expressed in adult muscle fibers, but is present in Pax7-
478 expressing satellite cells. Quiescent satellite cells are activated upon injury, proliferate,
479 differentiate, and ultimately provide new myonuclei for the regenerating fiber leading to Ulk1
480 expression in the regenerated muscle fiber. Additionally, following traumatic muscle injury there
481 are many other cell types that migrate into the injured territory to aid in muscle regeneration.
482 These include inflammatory cells such as neutrophils and macrophages, fibro-adipogenic
483 precursor cells (FAPs), fibroblasts, and endothelial cells all of which potentially express Ulk1
484 sufficient for autophagy induction (41). This premise is supported by our immunoblots showing
485 Ulk1 protein content within the injured limbs of Ulk1 MKO mice (Fig. 6). This is a clear
486 physiological limitation of this study and limits our ability to determine the necessity of Ulk1 for
487 mitochondrial remodeling after traumatic injury. To circumvent this problem for future
488 experiments, we are exploring the use of *Pax7^{CreER}* mouse lines to effectively knockout Ulk1 in
489 satellite cells and adult muscle fibers.

490 In this study, our finding that Ulk1 MKO impairs satellite cell proliferation raises an
491 intriguing question – how does muscle fiber autophagy indirectly affect satellite cell dynamics?

492 Satellite cells are essential stem cells for muscle regeneration and after traumatic injury (e.g.,
493 freeze injury), satellite cells exit quiescence and proliferate to form myoblasts (43). Myofiber-
494 derived FGF2 and FGF6 are important mitogens for satellite cells during muscle regeneration (1,
495 7, 11, 15, 28). One possibility is that Ulk1-dependent autophagy may be pivotal for FGF2/6
496 expression and secretion in damaged myofibers. Alternatively, Ulk1-dependent autophagy may
497 contribute to the degeneration of damaged myofibers by autophagy induced cell death, which
498 would be critical for setting the stage for satellite cell proliferation via timely recruitments of
499 macrophages and FAPs. No matter what mechanism is involved, the observations in this study
500 suggest an indirect positive influence of autophagy in myofibers on satellite cell proliferation,
501 which may be therapeutically targeted in the future for improving muscle regeneration.

502 In conclusion, this work advances the field in three substantive ways. First, physiological
503 muscle stressors that cause a decrease in muscle contractility and potentially result in
504 mitochondrial stress do not always elicit a decline in mitochondrial function, as assessed via
505 oxygen consumption. Second, autophagy flux does not scale to the increase in total autophagy
506 machinery that follows traumatic muscle injury, and this may represent a critical bottleneck to
507 address with targeted therapies to enhance the recovery of muscle function. Third, autophagy
508 appears to participate in the clearance of damaged mitochondria following traumatic injury in
509 line with what has been reported following non-injurious muscle stressors (20). Therefore, future
510 investigations into the role of autophagy following muscle stress associated with mitochondria
511 should strongly consider an evaluation of mitochondrial function to complement a localized
512 analysis of mitochondria stress and the use of a lysosomal inhibitor to determine autophagy flux.
513 Unfortunately, we were unable to fully determine the necessity of Ulk1 for timely recovery of
514 mitochondrial function due to the limitation of the mouse model; however, we are intrigued by

515 the strength deficits in the mice and potential crosstalk between Ulk1 in the adult muscle fiber
516 and satellite cells during muscle regeneration.

517 Acknowledgements

518 Research reported in this publication was supported by the National Institute of Arthritis and
519 Musculoskeletal and Skin Diseases of the National Institutes of Health under Award Number
520 1R01AR070178.

521 References

- 522 1. **Anderson JE, Mitchell CM, McGeachie JK, and Grounds MD.** The time course of
523 basic fibroblast growth factor expression in crush-injured skeletal muscles of SJL/J and BALB/c
524 mice. *Experimental cell research* 216: 325-334, 1995.
- 525 2. **Ato S, Makanae Y, Kido K, Sase K, Yoshii N, and Fujita S.** The effect of different
526 acute muscle contraction regimens on the expression of muscle proteolytic signaling proteins and
527 genes. *Physiological reports* 5: 2017.
- 528 3. **Baltgalvis KA, Call JA, Cochrane GD, Laker RC, Yan Z, and Lowe DA.** Exercise
529 training improves plantar flexor muscle function in mdx mice. *Med Sci Sports Exerc* 44: 1671-
530 1679, 2012.
- 531 4. **Call JA, Eckhoff MD, Baltgalvis KA, Warren GL, and Lowe DA.** Adaptive strength
532 gains in dystrophic muscle exposed to repeated bouts of eccentric contraction. *J Appl Physiol*
533 (1985) 111: 1768-1777, 2011.
- 534 5. **Call JA, Warren GL, Verma M, and Lowe DA.** Acute failure of action potential
535 conduction in mdx muscle reveals new mechanism of contraction-induced force loss. *J Physiol*
536 591: 3765-3776, 2013.
- 537 6. **Call JA, Wilson RJ, Laker RC, Zhang M, Kundu M, and Yan Z.** Ulk1-mediated
538 autophagy plays an essential role in mitochondrial remodeling and functional regeneration of
539 skeletal muscle. *Am J Physiol Cell Physiol* ajpcell.00348.02016, 2017.
- 540 7. **Chakkalakal JV, Jones KM, Basson MA, and Brack AS.** The aged niche disrupts
541 muscle stem cell quiescence. *Nature* 490: 355-360, 2012.
- 542 8. **Collins MA, An J, Peller D, and Bowser R.** Total protein is an effective loading control
543 for cerebrospinal fluid western blots. *Journal of neuroscience methods* 251: 72-82, 2015.
- 544 9. **Duguez S, Feasson L, Denis C, and Freyssenet D.** Mitochondrial biogenesis during
545 skeletal muscle regeneration. *American journal of physiology Endocrinology and metabolism*
546 282: E802-809, 2002.
- 547 10. **Egan DF, Shackelford DB, Mihaylova MM, Gelino S, Kohnz RA, Mair W, Vasquez**
548 **DS, Joshi A, Gwinn DM, Taylor R, Asara JM, Fitzpatrick J, et al.** Phosphorylation of ULK1
549 (hATG1) by AMP-activated protein kinase connects energy sensing to mitophagy. *Science (New*
550 *York, NY)* 331: 456-461, 2011.
- 551 11. **Floss T, Arnold HH, and Braun T.** A role for FGF-6 in skeletal muscle regeneration.
552 *Genes & development* 11: 2040-2051, 1997.

- 553 12. **Foltz SJ, Luan J, Call JA, Patel A, Peissig KB, Fortunato MJ, and Beedle AM.** Four-
554 week rapamycin treatment improves muscular dystrophy in a fukutin-deficient mouse model of
555 dystroglycanopathy. *Skeletal muscle* 6: 20, 2016.
- 556 13. **Garcia-Prat L, Martinez-Vicente M, Perdiguero E, Ortet L, Rodriguez-Ubreva J,**
557 **Rebollo E, Ruiz-Bonilla V, Gutarra S, Ballestar E, Serrano AL, Sandri M, and Munoz-**
558 **Canoves P.** Autophagy maintains stemness by preventing senescence. *Nature* 529: 37-42, 2016.
- 559 14. **Hardy D, Besnard A, Latil M, Jouvion G, Briand D, Thepenier C, Pascal Q, Guguin**
560 **A, Gayraud-Morel B, Cavaillon JM, Tajbakhsh S, Rocheteau P, et al.** Comparative Study of
561 Injury Models for Studying Muscle Regeneration in Mice. *PloS one* 11: e0147198, 2016.
- 562 15. **Kastner S, Elias MC, Rivera AJ, and Yablonka-Reuveni Z.** Gene expression patterns
563 of the fibroblast growth factors and their receptors during myogenesis of rat satellite cells. *The*
564 *journal of histochemistry and cytochemistry : official journal of the Histochemistry Society* 48:
565 1079-1096, 2000.
- 566 16. **Kim J, Kundu M, Viollet B, and Guan KL.** AMPK and mTOR regulate autophagy
567 through direct phosphorylation of Ulk1. *Nature cell biology* 13: 132-141, 2011.
- 568 17. **Klionsky DJ, Abdelmohsen K, Abe A, Abedin MJ, Abeliovich H, Acevedo Arozena**
569 **A, Adachi H, Adams CM, Adams PD, Adeli K, Adhietty PJ, Adler SG, et al.** Guidelines for
570 the use and interpretation of assays for monitoring autophagy (3rd edition). *Autophagy* 12: 1-
571 222, 2016.
- 572 18. **Kundu M, Lindsten T, Yang CY, Wu J, Zhao F, Zhang J, Selak MA, Ney PA, and**
573 **Thompson CB.** Ulk1 plays a critical role in the autophagic clearance of mitochondria and
574 ribosomes during reticulocyte maturation. *Blood* 112: 1493-1502, 2008.
- 575 19. **Kuznetsov AV, Veksler V, Gellerich FN, Saks V, Margreiter R, and Kunz WS.**
576 Analysis of mitochondrial function in situ in permeabilized muscle fibers, tissues and cells.
577 *Nature protocols* 3: 965-976, 2008.
- 578 20. **Laker RC, Drake JC, Wilson RJ, Lira VA, Lewellen BM, Ryall KA, Fisher CC,**
579 **Zhang M, Saucerman JJ, Goodyear LJ, Kundu M, and Yan Z.** Ampk phosphorylation of
580 Ulk1 is required for targeting of mitochondria to lysosomes in exercise-induced mitophagy.
581 *Nature communications* 8: 548, 2017.
- 582 21. **Le G, Lowe DA, and Kyba M.** Freeze Injury of the Tibialis Anterior Muscle. *Methods*
583 *Mol Biol* 1460: 33-41, 2016.
- 584 22. **Lovering RM, Roche JA, Bloch RJ, and De Deyne PG.** Recovery of function in
585 skeletal muscle following 2 different contraction-induced injuries. *Archives of physical medicine*
586 *and rehabilitation* 88: 617-625, 2007.
- 587 23. **Lynch GS, Hinkle RT, Chamberlain JS, Brooks SV, and Faulkner JA.** Force and
588 power output of fast and slow skeletal muscles from mdx mice 6-28 months old. *J Physiol* 535:
589 591-600, 2001.
- 590 24. **Magalhaes J, Fraga M, Lumini-Oliveira J, Goncalves I, Costa M, Ferreira R,**
591 **Oliveira PJ, and Ascensao A.** Eccentric exercise transiently affects mice skeletal muscle
592 mitochondrial function. *Applied physiology, nutrition, and metabolism = Physiologie appliquee,*
593 *nutrition et metabolisme* 38: 401-409, 2013.
- 594 25. **Marzetti E, Calvani R, Cesari M, Buford TW, Lorenzi M, Behnke BJ, and**
595 **Leeuwenburgh C.** Mitochondrial dysfunction and sarcopenia of aging: from signaling pathways
596 to clinical trials. *The international journal of biochemistry & cell biology* 45: 2288-2301, 2013.

- 597 26. **Molnar AM, Servais S, Guichardant M, Lagarde M, Macedo DV, Pereira-Da-Silva**
598 **L, Sibille B, and Favier R.** Mitochondrial H₂O₂ production is reduced with acute and chronic
599 eccentric exercise in rat skeletal muscle. *Antioxidants & redox signaling* 8: 548-558, 2006.
- 600 27. **Nichenko AS, Southern WM, Atuan M, Luan J, Peissig KB, Foltz SJ, Beedle AM,**
601 **Warren GL, and Call JA.** Mitochondrial maintenance via autophagy contributes to functional
602 skeletal muscle regeneration and remodeling. *Am J Physiol Cell Physiol* 311: C190-200, 2016.
- 603 28. **Olwin BB, and Hauschka SD.** Identification of the fibroblast growth factor receptor of
604 Swiss 3T3 cells and mouse skeletal muscle myoblasts. *Biochemistry* 25: 3487-3492, 1986.
- 605 29. **Pauly M, Daussin F, Burelle Y, Li T, Godin R, Fauconnier J, Koechlin-Ramonatxo**
606 **C, Hugon G, Lacampagne A, Coisy-Quivy M, Liang F, Hussain S, et al.** AMPK activation
607 stimulates autophagy and ameliorates muscular dystrophy in the mdx mouse diaphragm. *The*
608 *American journal of pathology* 181: 583-592, 2012.
- 609 30. **Ratray B, Caillaud C, Ruell PA, and Thompson MW.** Heat exposure does not alter
610 eccentric exercise-induced increases in mitochondrial calcium and respiratory dysfunction.
611 *European journal of applied physiology* 111: 2813-2821, 2011.
- 612 31. **Ratray B, Thompson M, Ruell P, and Caillaud C.** Specific training improves skeletal
613 muscle mitochondrial calcium homeostasis after eccentric exercise. *European journal of applied*
614 *physiology* 113: 427-436, 2013.
- 615 32. **Sandri M, Coletto L, Grumati P, and Bonaldo P.** Misregulation of autophagy and
616 protein degradation systems in myopathies and muscular dystrophies. *Journal of cell science*
617 126: 5325-5333, 2013.
- 618 33. **Silva LA, Bom KF, Tromm CB, Rosa GL, Mariano I, Pozzi BG, Tuon T, Stresck**
619 **EL, Souza CT, and Pinho RA.** Effect of eccentric training on mitochondrial function and
620 oxidative stress in the skeletal muscle of rats. *Brazilian journal of medical and biological*
621 *research = Revista brasileira de pesquisas medicas e biologicas* 46: 14-20, 2013.
- 622 34. **Southern WM, Nichenko AS, Shill DD, Spencer CC, Jenkins NT, McCully KK, and**
623 **Call JA.** Skeletal muscle metabolic adaptations to endurance exercise training are attainable in
624 mice with simvastatin treatment. *PLoS one* 12: e0172551, 2017.
- 625 35. **Vigelso A, Dybboe R, Hansen CN, Dela F, Helge JW, and Guadalupe Grau A.**
626 GAPDH and beta-actin protein decreases with aging, making Stain-Free technology a superior
627 loading control in Western blotting of human skeletal muscle. *J Appl Physiol (1985)* 118: 386-
628 394, 2015.
- 629 36. **Wagatsuma A, Kotake N, and Yamada S.** Muscle regeneration occurs to coincide with
630 mitochondrial biogenesis. *Molecular and cellular biochemistry* 349: 139-147, 2011.
- 631 37. **Wang X, Pickrell AM, Rossi SG, Pinto M, Dillon LM, Hida A, Rotundo RL, and**
632 **Moraes CT.** Transient systemic mtDNA damage leads to muscle wasting by reducing the
633 satellite cell pool. *Human Molecular Genetics* 22: 3976-3986, 2013.
- 634 38. **Warren GL, Ingalls CP, Lowe DA, and Armstrong RB.** Excitation-contraction
635 uncoupling: major role in contraction-induced muscle injury. *Exercise and sport sciences*
636 *reviews* 29: 82-87, 2001.
- 637 39. **Warren GL, Summan M, Gao X, Chapman R, Hulderman T, and Simeonova PP.**
638 Mechanisms of skeletal muscle injury and repair revealed by gene expression studies in mouse
639 models. *J Physiol* 582: 825-841, 2007.
- 640 40. **Wilson RJ, Drake JC, Cui D, Ritger ML, Guan Y, Call JA, Zhang M, Leitner LM,**
641 **Godecke A, and Yan Z.** Voluntary running protects against neuromuscular dysfunction
642 following hindlimb ischemia-reperfusion in mice. *J Appl Physiol (1985)* 126: 193-201, 2019.

- 643 41. **Wosczyzna MN, and Rando TA.** A Muscle Stem Cell Support Group: Coordinated
644 Cellular Responses in Muscle Regeneration. *Developmental cell* 46: 135-143, 2018.
- 645 42. **Xie L, Yin A, Nichenko AS, Beedle AM, Call JA, and Yin H.** Transient HIF2A
646 inhibition promotes satellite cell proliferation and muscle regeneration. *J Clin Invest* 2018.
- 647 43. **Yin H, Price F, and Rudnicki MA.** Satellite cells and the muscle stem cell niche.
648 *Physiological reviews* 93: 23-67, 2013.
- 649 44. **Zeitler AF, Gerrer KH, Haas R, and Jimenez-Soto LF.** Optimized semi-quantitative
650 blot analysis in infection assays using the Stain-Free technology. *Journal of microbiological*
651 *methods* 126: 38-41, 2016.
- 652